Biochimica et Biophysica Acta 1858 (2016) 123–129

Contents lists available at ScienceDirect

Biochimica et Biophysica Acta

journal homepage: www.elsevier.com/locate/bbamem

CNS myelin structural modification induced in vitro by phospholipases A2

Pablo J. Yunes Quartino [a], Julio M. Pusterla [a], Victor M. Galván Josa [b], Gerardo D. Fidelio [a], Rafael G. Oliveira [a,*]

[a] Departamento de Química Biológica-CIQUIBIC (CONICET), Facultad de Ciencias Químicas, Universidad de Nacional de Córdoba, Haya de la Torre S/N, X5000HUA, Córdoba, Argentina
[b] Consejo Nacional de Investigaciones Científicas y Técnicas (CONICET), FaMAF, Universidad Nacional de Córdoba, Argentina

ARTICLE INFO

Article history:
Received 30 June 2015
Received in revised form 22 October 2015
Accepted 23 October 2015
Available online 26 October 2015

Keywords:
Myelin
Phospholipases
Saxs
Demyelination
Langmuir monolayers

ABSTRACT

Myelin is the self-stacked membrane surrounding axons; it is also the target of several pathological and/or neurodegenerative processes like multiple sclerosis. These processes involve, among others, the hydrolytic attack by phospholipases. In this work we describe the changes in isolated myelin structure after treatment with several secreted PLA_2 ($sPLA_2$), by using small angle x-ray scattering (SAXS) measurements. It was observed that myelin treated with all the tested $sPLA_2$s (from cobra and bee venoms and from pig pancreas) preserved the lamellar structure but displayed an enlarged separation between membranes in certain zones. Additionally, the peak due to membrane asymmetry was clearly enhanced. The coherence length was also lower than the non-treated myelin, indicating increased disorder. These SAXS results were complemented by Langmuir film experiments to follow myelin monolayer hydrolysis at the air/water interface by a decrease in electric surface potential at different surface pressures. All enzymes produced hydrolysis with no major qualitative difference between the isoforms tested.

1. Introduction

Myelin is the membrane wrapping axons allowing for saltatory nerve conduction. It self-stacks in a unique way as a spiral structure. Due to this fact, the myelin structures from CNS and from PNS are among the best characterized natural membranes [1]. Myelin multilayers exhibit a rich phase behavior depending on the external conditions [2–4]. This behavior follows similar trends in nerves and in isolated membranes [5] as well as in monolayers at the air/water interface [6]. This makes purified myelin a convenient membrane model in order to study some processes of biological relevance, which otherwise are difficult to study in the nervous system in vivo.

Pathological, inflammatory and remodeling processes involve the attack against myelin by several factors like cells [7], autoantibodies [8], hydrolytic enzymes [7,9], among others. Secreted phospholipases A_2 ($sPLA_2$) comprise a set of compact enzymes (13–15 kDa) showing similarity in sequence and tertiary structure, requiring Ca^{2+} for hydrolytic activity [10]. These enzymes hydrolyze the *sn*-2 ester bond of substrate glycerophospholipids, yielding a lysophospholipid and a fatty acid [10]. In myelin membranes the glycerophospholipids represent a total mole fraction of ~0.3 [11].

There are proofs that different PLA_2s (not restricted to $sPLA_2$) act during myelin-related neurological diseases like multiple sclerosis or its laboratory model, the experimental autoimmune encephalomyelitis (EAE) [12,13]. PLA_2s affect myelin in other contexts, such as Wallerian degeneration, the process of breakdown and phagocytosis of myelin and axons distal to the site of a severe injury [14]. There is also current interest in cases of less severe injury such as the effect of PLA_2s against myelin in post trauma events of the spinal cord [15,16]. Additionally, virulence in specific strains causing amoebic (meningo) encephalitis was correlated to myelin degradation by PLA_2 secreted to the medium by the microorganism [17,18].

Besides, lysophospholipids, one of the two products of the PLA_2–catalyzed hydrolysis, are used as inducers of demyelination [19–22]. There still remains the question whether the role of lysophospholipids is mainly lytic or through a metabolic effect as second messengers [22].

Early biochemical work probed the activity of $sPLA_2$ against isolated myelin, showing that the main substrates are phosphatidylcholine, phosphatidylethanolamine, and phosphatidylserine, and the hydrolytic products remained associated to the membrane [23,24]. Additionally, no structural alteration in myelin was observed by TEM [24]. However, TEM induces artifacts and/or misinterpretations on myelin, as evidenced by studies of X-ray diffraction showing a series of alterations in its packing and structure at the different stages of specimen preparation for TEM [25]; this remained as an open problem without general

Abbreviations: CARS, coherent anti-Stokes Raman scattering; CNS, central nervous system; DPPC, 1,2-dipalmitoyl-sn-glycero-3-phosphocholine; EAE, experimental autoimmune encephalomyelitis; TEM, transmission electron microscopy; LysoPC, 1-palmitoyl-2-hydroxy-*sn*-glycero-3-phosphocholine; $sPLA_2$, secretory phospholipase A2; PNS, peripheral nervous system; SAXS, small angle x-ray scattering.

* Corresponding author.
E-mail address: oliveira@fcq.unc.edu.ar (R.G. Oliveira).

http://dx.doi.org/10.1016/j.bbamem.2015.10.017
0005-2736/

solution [26]. Thus, the significance of some observations performed with TEM comes into question. On the other hand, coherent anti-Stokes Raman scattering (CARS) microscopy showed that lysophosphatidylcholine, as well as externally administered cytosolic PLA_2 induced the swelling of myelin [22].

In this work we characterized $sPLA_2$-induced modifications on myelin organization as assessed by small angle X-ray scattering (SAXS). SAXS requires no further sample treatment after myelin isolation, and (contrary to TEM) preserves the aqueous environment (water and solutes) avoiding chemical modification. It also collects data over relatively big volumes, rendering a good statistical sampling. TEM, although visually rich, lacks all those benefits.

Additionally, we performed experiments on Langmuir monolayers of myelin at the air/water interface [6,27] to follow the $sPLA_2$ catalyzed hydrolysis by changes on electric surface potential [28,29].

2. Materials and methods

2.1. Chemicals

Highly purified myelin was prepared from bovine spinal cord according to [30]. Briefly, the purification protocol consisted of several osmotic shocks and direct as well as inverse sucrose gradient centrifugations to discard gray matter constituents according to density. After 3 final rinses in distilled water the myelin membranes were lyophilized and stored at −20 or −70 °C. Chemicals were of analytical grade and purchased from Merck (Germany). Myelin lipids were purified according to [31].

L-DPPC and D-DPPC were from Avanti Polar Lipids (Alabama, USA), $sPLA_2$s from the venom of bee and Cobra (*Naja naja*) were from Sigma Aldrich (USA), catalog numbers: P-6139, P-7778 respectively. $sPLA_2$ from pig pancreas (Lecitase 10L) was from Novonordisk (Denmark).

2.2. Hydrolysis product quantitation

The quantitation of released free fatty acids after incubation of myelin suspensions with $sPLA_2$ was performed using an enzyme-based colorimetric assay. For this, the HR Series NEFA-HR kit (Wako, Japan) was used. Myelin was suspended at 6 μg/μL, in a solution of 145 mM NaCl, 10 mM HEPES, 2 mM $CaCl_2$, pH = 7.4. $sPLA_2$ was added up to a concentration of 0.25 ng/μL (aprox. 17 nM) and 0.25 μg/μL (17 μM) for total hydrolysis condition. After the time of incubation with $sPLA_2$ (1 h or 12 h for total hydrolysis), the kit reagents were added following manufacturer's instructions. After this, the suspension was centrifuged 5 min at 12,000 × *g* and the absorbance of the supernatant at 550 nm was quantified. Calibration curve was made using the oleic acid solution provided in the kit. Controls included a no enzyme tube, and a mixture of the full reaction mixture (including color reagents) not subjected to incubation, in order to correct for non-enzymatic color or dispersion.

2.3. Small-angle X-ray scattering (SAXS)

SAXS was measured to determine the regular spacings *d* between bilayers of myelin membrane suspensions, $d = 2\pi/q$, where *q* is the scattering vector modulus $q = 4\pi\lambda^{-1} * (sin\ 2\theta/2)$ and 2θ is the scattering angle from the direct beam and λ is the X-ray wavelength. Measurements were performed at the SAXS2 beamline at LNLS (Campinas, Brazil). Lyophilized myelin was suspended at 6 mg/mL with a solution of NaCl 145 mM, Hepes 10 mM, $CaCl_2$ 2 mM pH = 7.4, and homogenized by extrusion (five times through a 26G needle fitted to a syringe). After this, the enzyme solution was added to a final concentration of 0.25 ng/μL and incubated for 1 h at 37 °C unless otherwise stated. Finally, the myelin suspension was filled into the sample holder between two mica plates for SAXS measurement. 1.488 Å radiation was used and the sample detector distance was ~1 m. For radial integration of the Debye–Scherrer rings on the 2D detector we employed the free software Fit2D V12.077 from Andy Hammersley at European Synchrotron Radiation Facility. Coherence lengths were estimated from the full width at half maximum of the major peak through the Scherrer equation or by fitting the data to a slab model. In some samples, sucrose 0.44 mM was added in order to avoid sample precipitation.

2.4. sPLA2-induced lipid and myelin monolayers hydrolysis followed by surface potential

Lyophilized myelin was hydrated in water at 1 mg/mL. When about to spread a monolayer at the air/water interface, 50 μL of that myelin aqueous suspension was added to 950 μL of chloroform : methanol 2:1 and immediately spread onto the surface of the aqueous phase. This was the same treatment given to a $sPLA_2$ treated sample before spreading. When using myelin lipids or DPPC, a chloroform–methanol 2:1 solution was prepared at 1 mg/mL and 0.5 mM respectively. Hamilton syringes were used in all cases for spreading.

Subphase composition was the same as the solution used for the suspension of myelin in the SAXS measurements, 145 mM NaCl, 10 mM Hepes, 2 mM $CaCl_2$, pH = 7.4. It was checked for the absence of surfactants by compression. Surface lateral pressure was followed by the Wilhelmy plate method using a Monofilmmeter built according to [32] by Film Lift, Mayer Feintechnique, (Göttingen, Germany). The surface potential was followed using a millivoltmeter with an air-ionizing ^{241}Am plate and Ag/AgCl electrode pair. Monolayer spreading was done on a 16 cm^2 trapezoidal trough with 18 mL, with constant magnetic stirring, at 25 ± 0.5 °C. The target surface pressure was reached at constant area by spreading up to the desired value. After 10 min of equilibration, enzyme injection was performed, up to a final concentration of 2 nM unless otherwise stated.

3. Results

3.1. Bulk whole myelin and $sPLA_2$

Fig. 1 shows SAXS measurements performed at 37 °C on myelin before and after treatment with three different $sPLA_2$s. Results are expressed as $I(q)$ (intensity) as a function of the scattering vector modulus *q*, (see point 2.3). Before the $sPLA_2$ injection, (upper black curve) a typical pattern for myelin, consisting of peaks around 0.8 and 1.6 nm^{-1} was observed. The ratio of positions of the diffraction peaks as whole numbers (i. e. 1 : 2 : …) revealed a lamellar phase [33]. The black curve indicates a major dominating lamellar phase with bilayers of ~7.85 nm periodicity [5,6]. After 1–2 h of incubation with $sPLA_2$s, the diffraction peaks split in two, with less sharp peaks at the original value ($q \approx 0.8$ and 1.6 nm^{-1}) and new peak positions (at $q \approx 0.6$ and 1.2 nm^{-1}) also in 1:2 ratio. This showed an additional lamellar spacing with a more expanded period, of around 10–11 nm. The enzymatic activity did not destroy the original lamellar structure even after 24 h incubation, but generated a partial change in its spacing. The analysis (by using Scherrer equation) of the shape profile of the native peak (0.8 nm^{-1}) rendered about 15 lamellar layers correlated before the $sPLA_2$ treatment (Fig. 1, inset); dropping to about half of that amount after $sPLA_2$ treatment.

Additional evidence of the persistence of lamellar structure/s was the behavior of the *I* at lower *q* values (below the position of the diffraction peaks), following a power decay according to $I \propto q^{-2}$. This is evident in the log–log graph of Fig. 2, where straight lines with different slopes were drawn as references. The one in blue corresponds to $I \propto q^{-2}$. The magenta line shows the constant value expected for globular micelles as is the case of lyso-phosphatidyl choline (lyso-PC). Finally the gray line shows the theoretical slope for the case of tubular micelles. Complete analysis of the data at low *q* values (the so-called Guinier region) is not possible in correlated systems such as myelin, which prevents radius of gyration and molecular weight determinations, however

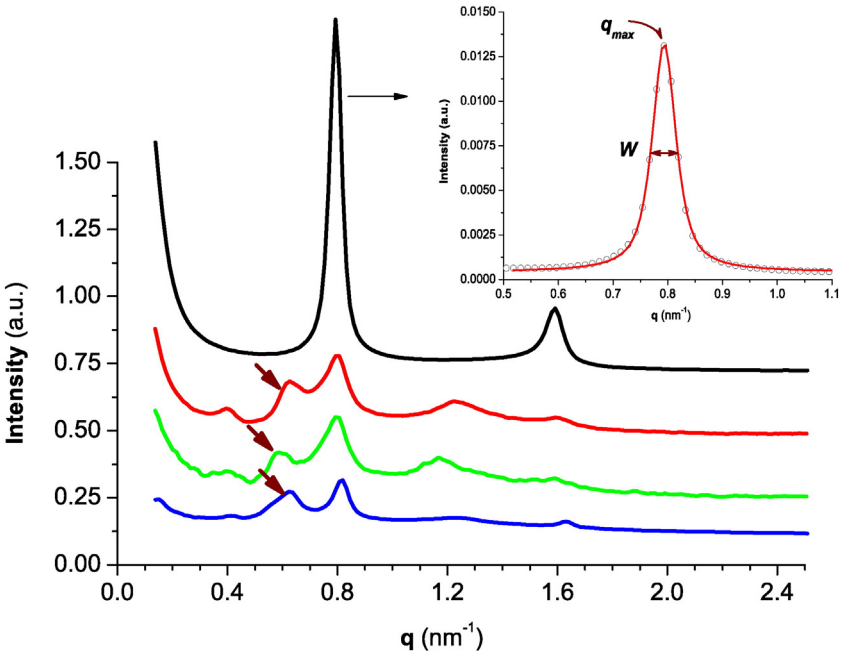

Fig. 1. Small angle X-ray diffraction of total myelin. Membranes before (upper black curve) and after exposure to $sPLA_2$s from different origin (color curves); from top to bottom: cobra venom (red), bee venom (green) and pig pancreas (blue) enzymes. Myelin showed the typical peak at q_{max} ~ 0.8 nm^{-1} (lamellar spacing of ~7.8 nm). A new expanded spacing was shown by the new peak at ~0.6 nm^{-1}(arrows). Inset, first order diffraction peak of the untreated myelin sample (black curve in main figure) fitted to a pseudo Voigt function, resulting in a coherent length of the myelin lamellar stack of 120 nm, which is about 15 lamellae, that is within the values found for native and isolated myelin. After $sPLA_2$ treatment, the coherence length decayed at about a half of the original one. W represents the full width at half maximum used for calculation of the coherence length.

dimensionality can still be derived. It is quite noticeable that I is proportional to q^{-2} and this fact is maintained after hydrolysis suggesting at least a not detectable change in the dimensionality (2D) of the lamellar arrangement.

Another new feature evident after $sPLA_2$ treatment is the appearance or enhancement of the peak located at ~0.4 nm^{-1}. This is exactly at half the value of the native, normal strong peak at 0.8 nm^{-1}, and corresponds to a duplication of the unit cell of the remaining native period, from 7.85 nm to 15.7 nm. Therefore, the enzymatic activity led to an increased asymmetry with a unit cell consisting of two bilayers, which could be related to the fact that exposed phospholipids were preferentially degraded (see below).

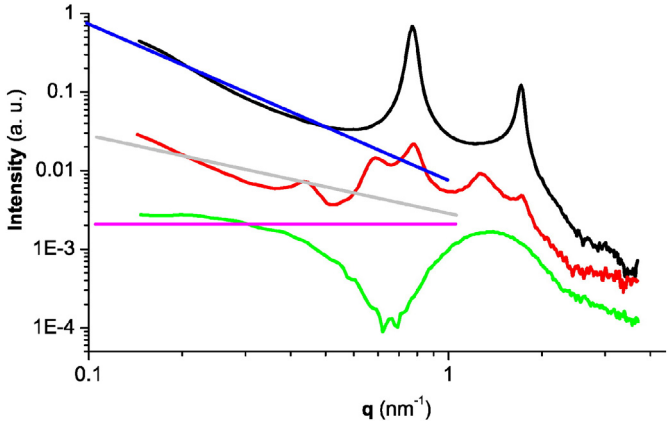

Fig. 2. Double logarithmic representation of SAXS data. Low q region is explored in the double logarithmic representation of the data (see text). Curves: non-treated myelin (black), $sPLA_2$-treated myelin as shown in Fig. 1 (red) and LysoPC (green). Both myelin curves match their slopes at low q with the blue reference line $I \propto q^{-2}$ (lamellar), while LysoPC, one product of the hydrolytic reaction, shows a relationship $I \propto q^{0}$ (a limiting constant value) as the magenta line (globular micelles). The gray line with $I \propto q^{-1}$ for tubular micelles does not match any set of data. The data at low q ($q < 0.3$–0.4 nm^{-1}) suggested that myelin membranes persisted after hydrolytic attack.

3.2. Hydrolysis product assay in myelin

After 1 h incubation at 37 °C, the pig pancreas $sPLA_2$ hydrolyzed 10 to 15% (0.04–0.06 μmol per mg myelin) of the total myelin hydrolyzable phospholipids whereas the cobra venom enzyme hydrolyzed 35 to 45%. The total hydrolyzable phospholipid was defined as the amount of quantitated fatty acid after 12 h incubation with $sPLA_2$ at 17 μM (1000-fold enzyme increase). These last facts are in agreement with previous results [23,24]. The free fatty acids before incubation with 17 nM $sPLA_2$ were below technique's sensitivity, however, after 12 h incubation the non-$sPLA_2$ added control sample showed detectable fatty acid production.

3.3. Bulk myelin lipid extract and $sPLA_2$

The purified myelin lipid extract in the presence of 2 mM $CaCl_2$ (needed for $sPLA_2$ catalyzed hydrolysis) showed a certain proportion of correlated lamellae as detected by clear Bragg peaks (Fig. 3, black curve). Under $sPLA_2$ hydrolysis these peaks shifted to lower q (Fig. 3, red curve), showing an analogous effect in the same direction as for whole myelin (Fig. 1). Nevertheless, the shift was reduced in comparison to whole myelin. The inset in Fig. 3 shows analogous behavior to whole myelin with $I(q)$ slopes proportional to q^{-2}, evidencing the lamellar arrangement even after PLA_2 treatment.

3.4. sPLA2-induced hydrolysis in Langmuir monolayers

To follow hydrolysis of myelin monolayers we turned to the continuous measurement of surface electric potential. As controls, we checked the action of $sPLA_2$ on L-DPPC monolayers and observed a drop in surface potential, as reported in earlier work [28]. This drop was absent in D-DPPC (non-hydrolysable enantiomer) monolayers after $sPLA_2$ injection, showing the enantiomeric selectivity of the enzyme and the

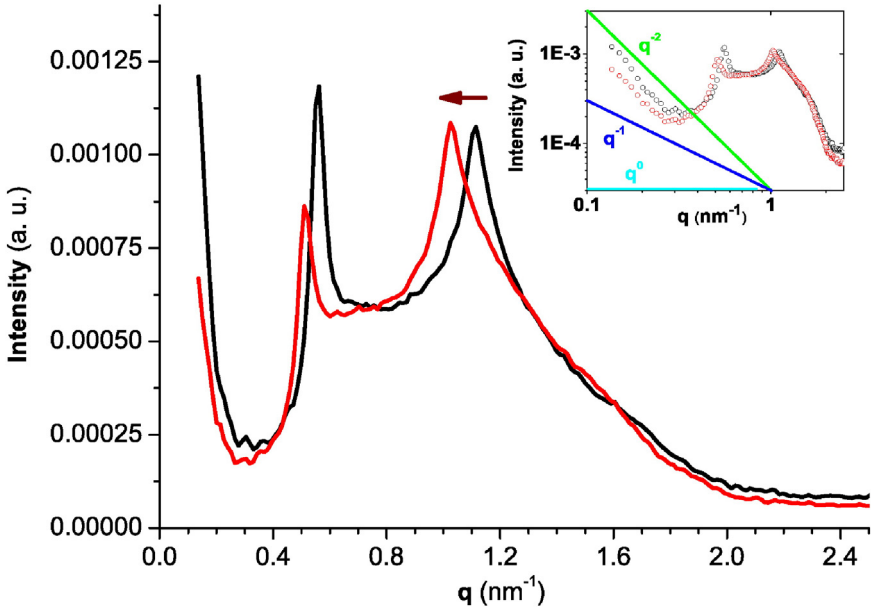

Fig. 3. Small angle x-ray diffraction of myelin lipids. Myelin lipids shifted to larger spacings (lower q, red curve, brown arrow) under $sPLA_2$ action. The inset shows a log–log representation of the data with lines of $I \propto q^{-2}$ (lamellar, green), $I \propto q^{-1}$ (tubular, blue) and $I \propto q^{-0}$ (globular micelles, cyan). The data at low q ($q < 0.3$) indicates that myelin lipid membranes persisted after hydrolytic attack, as observed for whole myelin.

lack of a major effect of the enzyme itself on surface potential (Fig S1). In the racemic (1:1) mixture the drop was proportional to the amount of L-DPPC.

Using the same technique we injected $sPLA_2$ from pig pancreas and cobra venom below myelin monolayers. The surface potential dropped very reproducibly and the rate of decay was inversely related to the original surface pressure (Fig. 4A).

This, together with the quantification of released free fatty acids of the bulk condition is an indication of the partial hydrolysis of phospholipids and the suitability of the surface potential (ΔV) to follow enzyme kinetics. Higher lateral surface pressure extended the ΔV equilibration time. At 19 $mN \cdot m^{-1}$ the equilibrium was reached in 10 min, but at 38 $mN \cdot m^{-1}$ the equilibrium was reached in about 1 h (Fig. 4A). This is the normal trend found for $sPLA_2$s. The surface pressure showed a less obvious and retarded decrease making it impractical to follow as a reaction indicator. This suggests that the products of hydrolysis were still remaining in the monolayer in good proportion, analogous to the case of bulk myelin membranes in our and other's works [23].

In other experiments we incubated myelin in bulk with $sPLA_2$ before monolayer spreading. Then, after formation of monolayer of that $sPLA_2$-treated myelin and subsequent enzyme injection, the drop in surface potential was around 40% of the drop seen when the myelin was not pre-treated with $sPLA_2$ (Fig. 4B). This would reflect the preservation of some phospholipids not accessible to the enzyme until spreading, as suggested by the increased asymmetry in SAXS results. When a lipid extract from myelin was spread as monolayer (Fig. 5), the surface potential drop upon hydrolysis was greater than whole myelin (Fig. 4), and the cobra venom $sPLA_2$ (Fig. 5A) was clearly more active than the pancreatic one (Fig. 5B). This was also the case with whole extracted myelin and was in accordance to the bulk assay quantitation of released fatty acids (data not shown).

4. Discussion

4.1. Whole myelin

The experimental decays of intensity at q values below the first diffraction peaks ($q < 0.3$–0.6 nm^{-1}) matched the one corresponding to a planar (lamellar) structure. If micelles appeared after hydrolysis, (as is normally the case for pure fatty acids, as well as pure lysophospholipids) a plateau in $I(q)$ would be expected for these structures and consequently a decay in the slope at low q values, which was not the case. This fact supports the idea that the hydrolytic products remained in the membrane, which agrees with the original determinations based in centrifugation experiments [23,24]. Then we agree with the seminal work in that the membrane planar structure is maintained after $sPLA_2$ digestion. But we disagree with the previously reported lack of effect on myelin lamellae packing [24].

The novelty in this work is to show a defined, partial separation in quantitative terms (of about 1.5–2.5 nm) between correlated myelin lamellae after $sPLA_2$ treatment, and that this did not occur over the entire membrane surface. This was accompanied by an increased asymmetry deduced by the appearance of the peak at 0.4 nm^{-1} (period duplication). We speculate that this separation should be more pronounced in the extracellular side of isolated myelin. The peak at 0.4 nm^{-1} is evident in nerve myelin but tends to be lower or absent after isolation [5], getting stronger whenever there is a splitting of the major peak at 0.8 nm^{-1} by any given circumstance [4,6].

The three $sPLA_2$s we tested displayed the same effect on myelin, leading to a new expanded period that could have physio-pathological relevance since it disturbs the packing status of myelin. Adhesion between myelin layers plays an important role on myelin stability and opposes the characteristic demyelination of several myelin altered states. Demyelination is preceded by loss of membrane adhesion, swelling, vesiculation, and finally myelin disintegration [8,19]; clearly PLA_2s could be responsible for some of the first steps.

In the past it was postulated that even if $sPLA_2$s chemically degraded myelin, this would not affect the ultrastructure as seen by TEM [24]. Only when $sPLA_2$ addition was combined with protease (trypsin), a membrane decoupling was observed by TEM [24]. In this regard it was also shown by low-angle X-ray diffraction that the action of proteases (trypsin and Pronase, separately) induce remodeling in myelin [34], although with some discrepancies [24,35]. The observation that $sPLA_2$ does not alter the myelin packing is quite surprising if we take into account that one of the hydrolytic products (lysophospholipid) is used to induce demyelination from long time ago and it was observed an extensive myelin reorganization after its intraneural injection [19,20]. Lysophospholipids are still extensively employed as a model to study

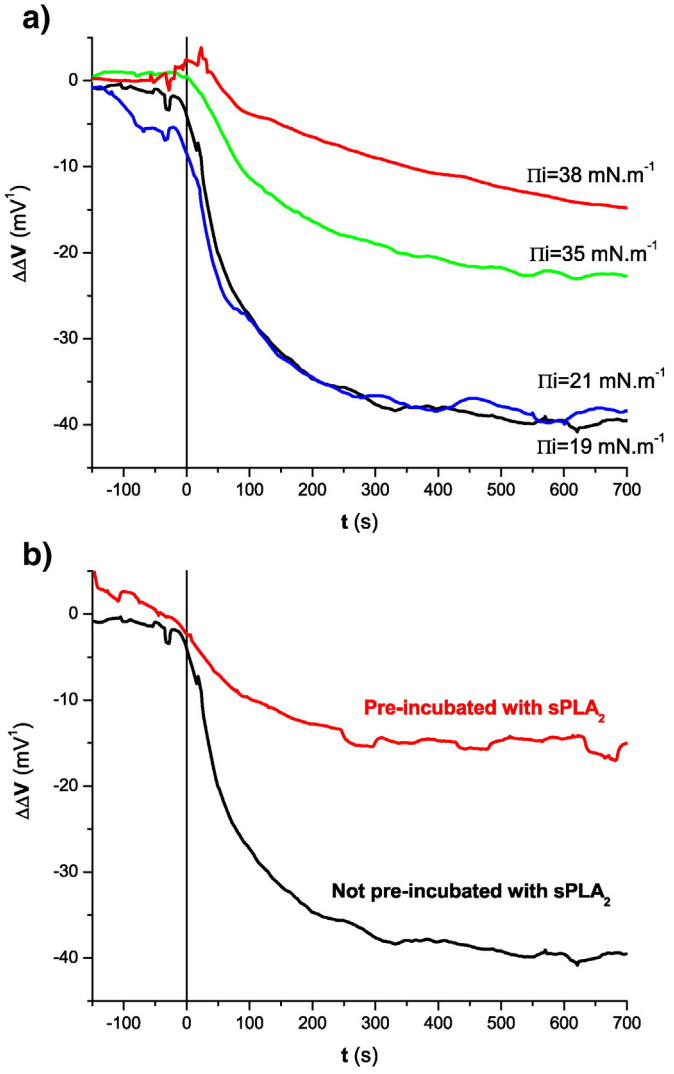

Fig. 4. Surface potential in whole myelin monolayers after $sPLA_2$ injection. (A) Effect of injection (t = 0 s) of cobra venom $sPLA_2$ (2 nM) on the surface potential difference (ΔΔV) changes at different initial surface pressure. At higher surface pressure (Πi = 38 mN·m^{-1}), the drop rate was reduced (red curve). (B) The drop was lower (~50%) in myelin pre-treated with $sPLA_2$ before spreading, showing the partial digestion of the membranes, measurements at 19 mN·m^{-1}.

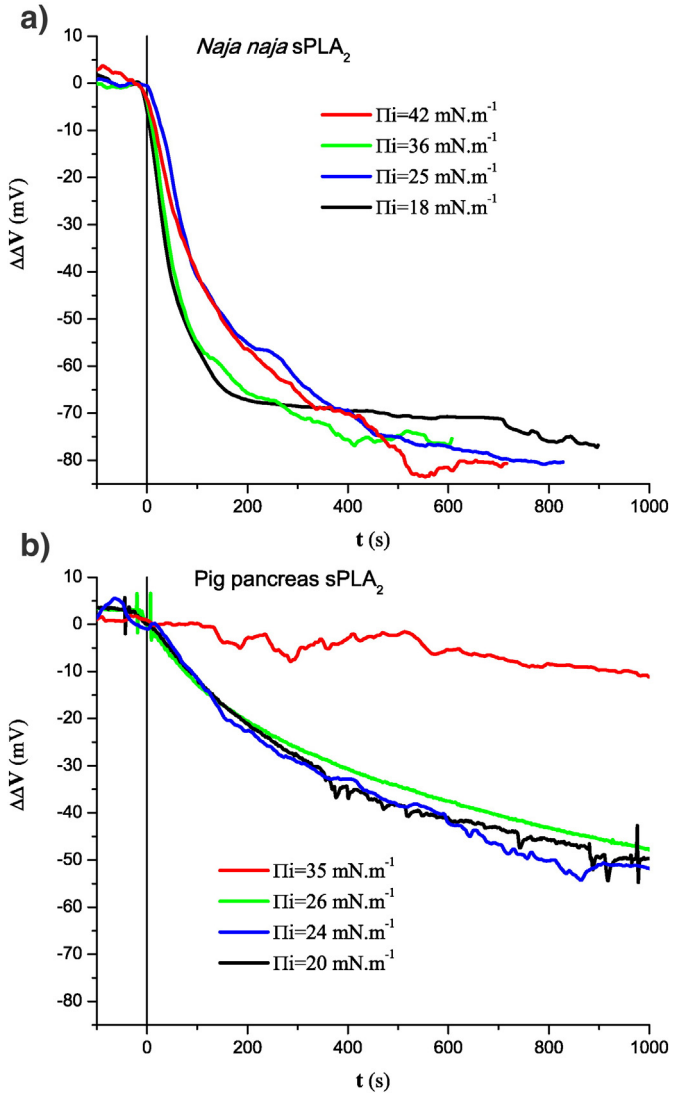

Fig. 5. Surface potential difference in myelin lipids monolayers after $sPLA_2$ injection. The surface potential drop (ΔΔV) appeared as a general phenomenon. In fact, in this case the surface potential drop is even greater than in whole myelin. (A) 15 nM cobra venom $sPLA_2$ (B) 15 nM $sPLA_2$ from pig pancreas, produced a less pronounced ΔΔV drop rate, and a notably slower drop at 35 mN·m^{-1} (red line).

demyelination and post demyelination effects, like remyelination [21]. We speculate that a possible reason for the discrepancy could be the fact that it was shown that TEM specimen preparation leads to artifacts with shrinking of the physiological states of myelin as assessed by X-ray diffraction [25]. Even in early times it was accepted that shrinking is a common phenomenon in myelin TEM preparations [36]. This artifact is absent in X-ray observations. Shrinking could compensate or obscure the expansion of the membranes in the particular conditions on which PLA_2 is assayed. More recently, it was demonstrated an increased swelling and disorder of myelin induced by PLA_2s and lysophospholipids by using CARS microscopy [22]. In this work we showed evidence of the structural change induced by different $sPLA_2$s by using SAXS and following Debye–Scherrer rings shifts and changes in peak profile related to coherence length by the Scherrer equation. The decrease in coherence length is indicative of fewer correlated membranes and thus of increased disorder. The spacing appeared to be bimodal, part retained the physiological value but other part was expanded by about 2 nm. Additionally, there was an increment in the asymmetry of the native period, as detected by the appearance of a discernible peak at 0.4 nm^{-1}. This peak marks the natural asymmetry of the native membrane, but is more difficult to observe in isolated CNS myelin [5,37]. In our case this increment was probably linked to the changes in composition [38]. Similar period duplication has been observed in simpler systems consisting of dipalmitoylphosphatidylcholine (DPPC) mixed with its hydrolysis products [38] and reflects the asymmetry of the bilayer. In myelin this could be due to increased asymmetry between the exposed and hydrolyzed (outer) monolayer and the non-exposed (inner) monolayer of the membrane bilayer. So far, no general rule can be extracted about the response of myelin to enzymes regarding the change in symmetry; for instance exposition to proteases decreases the PNS myelin asymmetry [34] which is the opposite to the results with $sPLA_2$.

We speculate that the decoupling of membranes in whole myelin can be due to increased LysoPC and/or increment of negative surface charge density due to fatty acids generation. The shift of the peak and the decoupling was weaker in isolated lipids as compared to whole myelin, but it happened over the entire sample. It should be taken into account that most probably the shift on lipids was not so noticeable because there was already (prior to $sPLA_2$ hydrolysis) a big amount (around 10 mol%) of anionic lipids [11] and because the new generated charge density can dilute over all the lipidic membrane.

4.2. Surface potential and PLA_2 specificity

Electrostatic surface potential differences (ΔΔV) is a proved method to follow the hydrolysis in Langmuir monolayers [28,29,39]. After enzyme injection below myelin monolayers at the air/water interface, ΔΔV were very similar for both paradigmatic enzymes, the one from pig pancreas, and from cobra venom, after 1 h incubation. Cobra venom $sPLA_2$ displayed consistently greater rates of ΔΔV drop at all surface pressures. However, we concluded that after enough time (1 h to 2 h incubation, depending on the initial surface pressure), both enzymes induced equal ΔΔV value.

In order to help to rationalize our observations in whole myelin, we performed the same study on two simpler substrates. One, a purified myelin lipids extract (no protein) and two, pure single lipids (L-DPPC and D-DPPC) and its racemic mixture. Purified myelin lipids showed also a drop in surface potential (Fig. 5) as did L-DPPC, but not D-DPPC (Fig S1). It should be taken into account that the binding affinity of $sPLA_2$s for the D-enantiomer monolayer equals that of the L phospholipid [40]. From analysis of the racemic mixture it was evident that depolarization was proportional to the density of substrate. Therefore, ΔΔV could be used as a measure of the phospholipid hydrolysis in these simpler systems.

In our SAXS determinations we did not follow the continuous process of the myelin modification, rather its initial and final states (the new expanded and more asymmetric state of myelin) which produced the same SAXS spectra for all the three tested enzymes. Nevertheless, it is known that the different $sPLA_2$s assayed could have different kinetics and efficiency in the hydrolytic process. These possible differences were analyzed here in Langmuir monolayer experiments. These secreted enzymes generally display great activity [41] at the physiological pH of the extracellular side of the CNS, which is around 7.4 [42].

Different $sPLA_2$s have different preference for substrates, but they also differ on the lateral molecular packing (followed by surface pressure Π) at which they are able to efficiently hydrolyze pure phospholipid Langmuir monolayers at the air/water interface. For instance, pig pancreas (digestive) $sPLA_2$ shows a markedly lower value of lateral pressure for pure short chain PCs films at which the optimum hydrolysis of monolayers is attained when compared with both, bee venom and cobra venom $sPLA_2$, having an almost null activity at 20 $mN \cdot m^{-1}$ [43,44]. Although cobra venom $sPLA_2$ still produced a faster hydrolysis at all pressures at the same bulk concentration, the difference with the pancreatic enzyme was not as sharp as reported for pure PC. Consistently, pancreatic $sPLA_2$ also hydrolyzed myelin bilayers that, according to our previous work have high molecular lateral packing, equivalent to the one near the monolayer collapse [6,45].

4.3. PLA_2 and myelin damage/remodeling

PLA_2s are known to be key participants in demyelination processes [7], like multiple sclerosis or its laboratory model, the EAE [12,13]. Additionally, it is well known that macrophages (and other cells) are commonly located at places of myelin injury and these cells are able to secrete PLA_2s [46] which are often associated to inflammatory processes. In all the general histo-morphological routes toward demyelination (stripping, dying back, vesiculation, phagocytosis [47]) the destabilization of the apposition between the membranes appears to be an early requisite.

PLA_2s affect myelin also in Wallerian degeneration [14] and in cases of less severe injury such as post trauma events of the spinal cord [15,16]. In other scenarios, like amoebic (meningo) encephalitis infection, PLA_2 appear to be a determinant factor, as virulence is linked to PLA_2 activity in secreted medium [18]. In fact, demyelination by Naegleria fowleri proceeds via phospholipolytic attack as the main factor [17]. Additionally, lysophospholipid, are used as inducers of demyelination [19–22].

In our work we clearly showed that PLA_2s (beyond its probed capability to chemically degrade myelin molecular constituents) are able to induce an increased and defined separation between myelin membranes, which could represent one of the first steps on myelin destabilization, turning it more accessible to other (bio)chemical agents.

5. Conclusion

We examined myelin periodicity incubated with different secreted phospholipases A_2 by employing SAXS. As a result, myelin qualitatively preserved its lamellar structure, part of myelin kept the normal periodicity but other part expanded, with only a fraction of phospholipids being actually degraded. Even the paradigmatic non-venom pancreatic phospholipase attacked myelin. This serves as an indication that is likely that even not very potent phospholipases could produce structural changes if acting on myelin, loosening its packing.

Conflict of interest

The authors declare no conflict of interest.

Acknowledgments

This work was supported by grants from CONICET (PIP 2012-14 #11220110100624), SeCyT (UNC) (2014-2015 203/14) and FonCyT (Argentina) (PICT 2012-2583). We acknowledge the Brazilian Synchrotron Light Laboratory for beamtimes at SAXS-2 beamline under research proposals SAXS1-10716 and SAXS1-13462. P.J.Y.Q. was a recent a fellow from CONICET and now is under contract with the UNC. J.M.P. is a doctoral fellow from CONICET. V.M.G.J., G.D.F and R.G.O. are members of the Scientific Research Career (CIC) from CONICET.

References

[1] H. Inouye, D.A. Kirschner, Myelin: a one-dimensional biological "crystal" for X-Ray and neutron scattering, in: J.S.a.P., Riccio (Eds.), Molecules: Nucleation, Aggregation and Crystallization, beyond medical and other implications, World Scientific Publishing Co, New Jersey 2009, pp. 75–94.
[2] C.J. Hollingshead, D.L. Caspar, V. Melchior, D.A. Kirschner, Compaction and particle segregation in myelin membrane arrays, J. Cell Biol. 89 (1981) 631–644.
[3] V. Melchior, C.J. Hollingshead, D.L. Caspar, Divalent cations cooperatively stabilize close membrane contacts in myelin, Biochim. Biophys. Acta 554 (1979) 204–226.
[4] C.R. Worthington, T.J. McIntosh, An X-ray study of the condensed and separated states of sciatic nerve myelin, Biochim. Biophys. Acta 436 (1976) 707–718.
[5] H. Inouye, J. Karthigasan, D.A. Kirschner, Membrane structure in isolated and intact myelins, Biophys. J. 56 (1989) 129–137.
[6] R.G. Oliveira, E. Schneck, S.S. Funari, M. Tanaka, B. Maggio, Equivalent aqueous phase modulation of domain segregation in myelin monolayers and bilayer vesicles, Biophys. J. 99 (2010) 1500–1509.
[7] M.L. Cuzner, W.T. Norton, Biochemistry of demyelination, Brain Pathol. 6 (1996) 231–242.
[8] C.P. Genain, B. Cannella, S.L. Hauser, C.S. Raine, Identification of autoantibodies associated with myelin damage in multiple sclerosis, Nat. Med. 5 (1999) 170–175.
[9] B. Maggio, F.A. Cumar, Experimental allergic encephalomyelitis: dissociation of neurological symptoms from lipid alterations in brain, Nature 253 (1975) 364–365.
[10] R.H. Schaloske, E.A. Dennis, The phospholipase A2 superfamily and its group numbering system, Biochim. Biophys. Acta 1761 (2006) 1246–1259.
[11] R.G. Oliveira, R.O. Calderon, B. Maggio, Surface behavior of myelin monolayers, Biochim. Biophys. Acta 1370 (1998) 127–137.
[12] T.J. Cunningham, L. Yao, M. Oetinger, L. Cort, E.P. Blankenhorn, J.I. Greenstein, Secreted phospholipase A2 activity in experimental autoimmune encephalomyelitis and multiple sclerosis, J. Neuroinflammation 3 (2006) 26.
[13] A. Kalyvas, C. Baskakis, V. Magrioti, V. Constantinou-Kokotou, D. Stephens, R. Lopez-Vales, J.Q. Lu, V.W. Yong, E.A. Dennis, G. Kokotos, S. David, Differing roles for members of the phospholipase A2 superfamily in experimental autoimmune encephalomyelitis, Brain 132 (2009) 1221–1235.
[14] S. De, M.A. Trigueros, A. Kalyvas, S. David, Phospholipase A2 plays an important role in myelin breakdown and phagocytosis during Wallerian degeneration, Mol. Cell. Neurosci. 24 (2003) 753–765.
[15] S. David, A.D. Greenhalgh, R. Lopez-Vales, Role of phospholipase A2s and lipid mediators in secondary damage after spinal cord injury, Cell Tissue Res. 349 (2012) 249–267.
[16] N.K. Liu, X.M. Xu, Phospholipase A2 and its molecular mechanism after spinal cord injury, Mol. Neurobiol. 41 (2010) 197–205.

[17] Y. Gutierrez, Diagnostic pathology of parasitic infections with clinical correlations, 2nd ed. Oxford University Press, 2000.
[18] R.M. Hysmith, R.C. Franson, Degradation of human myelin phospholipids by phospholipase-enriched culture media of pathogenic Naegleria fowleri, Biochim. Biophys. Acta 712 (1982) 698–701.
[19] S.M. Hall, N.A. Gregson, The in vivo and ultrastructural effects of injection of lysophosphatidyl choline into myelinated peripheral nerve fibres of the adult mouse, J. Cell Sci. 9 (1971) 769–789.
[20] N.A. Gregson, S.M. Hall, A quantitative analysis of the effects of the intraneural injection of lysophosphatidyl choline, J. Cell Sci. 13 (1973) 257–277.
[21] A.M. Adamo, Nutritional factors and aging in demyelinating diseases, Genes Nutr 9 (2014) 360.
[22] Y. Fu, H. Wang, T.B. Huff, R. Shi, J.X. Cheng, Coherent anti-Stokes Raman scattering imaging of myelin degradation reveals a calcium-dependent pathway in lyso-PtdCho-induced demyelination, J. Neurosci. Res. 85 (2007) 2870–2881.
[23] E. Coles, D.L. McIlwain, M.M. Rapport, The activity of pure phospholipase A2 from Crotalus atrox venom on myelin and on pure phospholipids, Biochim. Biophys. Acta 337 (1974) 68–78.
[24] N.L. Banik, K. Gohil, A.N. Davison, The action of snake venom, phospholipase A and trypsin on purified myelin in vitro, Biochem. J. 159 (1976) 273–277.
[25] D.A. Kirschner, C.J. Hollingshead, Processing for electron microscopy alters membrane structure and packing in myelin, J. Ultrastruct. Res. 73 (1980) 211–232.
[26] H.K. Feirabend, P. Kok, H. Choufoer, S. Ploeger, Preservation of myelinated fibers for electron microscopy: a qualitative comparison of aldehyde fixation, microwave stabilisation and other procedures all completed by osmication, J. Neurosci. Methods 55 (1994) 137–153.
[27] C.M. Rosetti, B. Maggio, R.G. Oliveira, The self-organization of lipids and proteins of myelin at the membrane interface. Molecular factors underlying the microheterogeneity of domain segregation, Biochim. Biophys. Acta 1778 (2008) 1665–1675.
[28] G. Colacicco, Significance of surface potential measurements on lipid monolayers during action of phospholipase A on lecithins, Nature 233 (1971) 202–204.
[29] K. Mircheva, T. Ivanova, I. Panaiotov, R. Verger, Hydrolysis of mixed monomolecular films of tricaprylin/dilauroylphosphatidylcholine by lipase and phospholipase A(2), Colloids Surf. B: Biointerfaces 86 (2011) 71–80.
[30] J.E. Haley, F.G. Samuels, R.W. Ledeen, Study of myelin purity in relation to axonal contaminants, Cell. Mol. Neurobiol. 1 (1981) 175–187.
[31] C.M. Rosetti, R.G. Oliveira, B. Maggio, The Folch–Lees proteolipid induces phase coexistence and transverse reorganization of lateral domains in myelin monolayers, Biochim. Biophys. Acta 1668 (2005) 75–86.
[32] P. Fromherz, Instrumentation for handling monomolecular films at an air–water interface, Rev. Sci. Instrum. 46 (1975) 1380–1385.
[33] T. Heimburg, Thermal Biophysics of Membranes, Wiley-VCH, Weinheim, 2007.
[34] C.R. Worthington, T.J. McIntosh, S. Lalitha, An X-ray study of the effect of enzymes on frog sciatic nerve myelin, Arch. Biochem. Biophys. 201 (1980) 429–436.
[35] J.G. Wood, R.M. Dawson, H. Hauser, Effect of proteolytic attack on the structure of CNS myelin membrane, J. Neurochem. 22 (1974) 637–643.
[36] H. Fernandez-Moran, J.B. Finean, Electron microscope and low-angle X-ray diffraction studies of the nerve myelin sheath, J. Biophys. Biochem. Cytol. 3 (1957) 725–748.
[37] J. Sedzik, A.D. Toews, A.E. Blaurock, P. Morell, Resistance to disruption of multilamellar fragments of central nervous system myelin, J. Neurochem. 43 (1984) 1415–1420.
[38] S.S. Funari, G. Rapp, F. Richter, Double-bilayer: a new phase formed by lysophospholipids and the corresponding fatty acid, Quim. Nova 32 (2009) 908–912.
[39] A. Hughes, The action of snake venoms on surface films, Biochem. J. 29 (1935) 437–444.
[40] P.P. Bonsen, G.H. de Haas, W.A. Pieterson, L.L. van Deenen, Studies on phospholipase A and its zymogen from porcine pancreas. IV. The influence of chemical modification of the lecithin structure on substrate properties, Biochim. Biophys. Acta 270 (1972) 364–382.
[41] D.A. Six, E.A. Dennis, The expanding superfamily of phospholipase A(2) enzymes: classification and characterization, Biochim. Biophys. Acta 1488 (2000) 1–19.
[42] M.A. Friese, M.J. Craner, R. Etzensperger, S. Vergo, J.A. Wemmie, M.J. Welsh, A. Vincent, L. Fugger, Acid-sensing ion channel-1 contributes to axonal degeneration in autoimmune inflammation of the central nervous system, Nat. Med. 13 (2007) 1483–1489.
[43] R.A. Demel, W.S. Geurts van Kessel, R.F. Zwaal, B. Roelofsen, L.L. van Deenen, Relation between various phospholipase actions on human red cell membranes and the interfacial phospholipid pressure in monolayers, Biochim. Biophys. Acta 406 (1975) 97–107.
[44] P.J. Yunes Quartino, J.L. Barra, G.D. Fidelio, Cloning and functional expression of secreted phospholipases A(2) from Bothrops diporus (Yarara Chica), Biochem. Biophys. Res. Commun. 427 (2012) 321–325.
[45] R.G. Oliveira, B. Maggio, Surface behavior, microheterogeneity and adsorption equilibrium of myelin at the air-water interface, Chem. Phys. Lipids 122 (2003) 171–176.
[46] P.D. Wightman, M.E. Dahlgren, P. Davies, R.J. Bonney, The selective release of phospholipase A2 by resident mouse peritoneal macrophages, Biochem. J. 200 (1981) 441–444.
[47] H. Lassmann, H. Wekerle, A.C.C.L.M.M.N.S. Wekerle, Chapter 12 — the pathology of multiple sclerosis, McAlpine's Multiple Sclerosis, fourth editionChurchill Livingstone, Edinburgh 2006, pp. 557–599.